molecular pharmaceutics

Article

pubs.acs.org/molecularpharmaceutics

Phosphorus Dendrimers Affect Alzheimer's ($A\beta_{1-28}$) Peptide and MAP-Tau Protein Aggregation

Tomasz Wasiak,[†] Maksim Ionov,[†] Krzysztof Nieznanski,[‡] Hanna Nieznanska,[‡] Oxana Klementieva,[§] Maritxell Granell,[§] Josep Cladera,[§] Jean-Pierre Majoral,[∥] Anne Marie Caminade,[∥] and Barbara Klajnert*[,†]

[†]Department of General Biophysics, University of Lodz, Poland

[‡]Department of Biochemistry, Nencki Institute of Experimental Biology, Warsaw, Poland

[§]Department of Biochemistry and Molecular Biology, Autonomous University of Barcelona, Spain

[∥]Laboratoire de Chimie de Coordination du CNRS, Toulouse, France

ABSTRACT: Alzheimer's disease (AD) is characterized by pathological aggregation of β-amyloid peptides and MAP-Tau protein. β-Amyloid ($A\beta$) is a peptide responsible for extracellular Alzheimer's plaque formation. Intracellular MAP-Tau aggregates appear as a result of hyperphosphorylation of this cytoskeletal protein. Small, oligomeric forms of $A\beta$ are intermediate products that appear before the amyloid plaques are formed. These forms are believed to be most neurotoxic. Dendrimers are highly branched polymers, which may find an application in regulation of amyloid fibril formation. Several biophysical and biochemical methods, like circular dichroism (CD), fluorescence intensity of thioflavin T and thioflavin S, transmission electron microscopy, spectrofluorimetry (measuring quenching of intrinsic peptide fluorescence) and MTT-cytotoxicity assay, were applied to characterize interactions of cationic phosphorus-containing dendrimers of generation 3 and generation 4 (CPDG3, CPDG4) with the fragment of amyloid peptide ($A\beta_{1-28}$) and MAP-Tau protein. We have demonstrated that CPDs are able to affect β-amyloid and MAP-Tau aggregation processes. A neuro-2a cell line (N2a) was used to test cytotoxicity of formed fibrils and intermediate products during the $A\beta_{1-28}$ aggregation. It has been shown that CPDs might have a beneficial effect by reducing the system toxicity. Presented results suggest that phosphorus dendrimers may be used in the future as agents regulating the fibrilization processes in Alzheimer's disease.

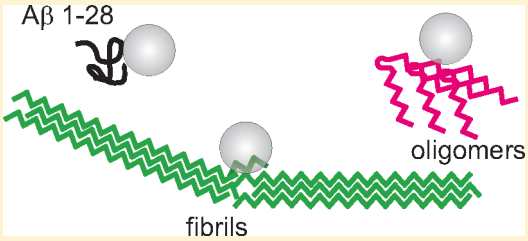

KEYWORDS: *phosphorus dendrimers, β-amyloid, MAP-Tau protein, fibril formation, amyloid peptide, aggregation, ThT assay, ThS assay, cytotoxicity*

INTRODUCTION

Pathological aggregation of proteins that leads to creation of amyloid fibrils is related to numerous human disorders, such as Alzheimer's and Parkinson's diseases, type II diabetes, and Creutzfeldt–Jakob disease.[1,2] In the case of neurodegenerative disorders, pathogenesis is strictly related to the accumulation of neurotoxic forms. Independently of amino acid sequence and the type of the disease there is a lot of evidence that oligomer forms are more toxic than mature fibrils.[3−7] Alzheimer's disease (AD) is the most frequent cause of memory loss and dementia in the elder human population. AD is characterized by loss of neurons and synapses in the cerebral cortex and certain subcortical regions.[8] A central role in the pathogenesis of AD is played by β-amyloid, a low molecular mass peptide (39- to 43-amino acid sequences), a proteolytic product of a high molecular mass amyloid precursor protein (APP) by enzymatic cleavage by β-secretases and γ-secretases.[9−11] β-Amyloid is released from neurons, skin and intestine cells and circulates in blood and cerebrospinal fluid.[12] In the Alzheimer's brain the transport across a blood–brain barrier is unsettled, and that results in accumulation and aggregation of the peptide. The process of aggregation can be followed by observation of changes in the secondary structure from unordered and α-helical ones to β-sheet-rich.[13,14] The mechanism of $A\beta$ toxicity may involve generation of reactive oxygen species, mitochondria damage and destabilization of intercellular calcium (Ca^{2+}) homeostasis.[15−17]

The second hallmark of AD is a manifestation of neurofibrillar tangles (NTFs) composed of hyperphosphorylated MAP-Tau protein aggregates.[18] MAP-Tau is a well soluble protein and in physiological conditions hardly shows a tendency to aggregate to insoluble fibers characteristic for the AD brain. MAP-Tau plays an important role in regulating microtubule stability and the rate of microtubule assembly, which is involved in numerous cellular processes such as maintaining a cell shape. The pathological aggregation is correlated with hyperphosphorylation of MAP-Tau in neurons and glia.[19] Hyperphosphorylated MAP-Tau is unable to bind to

Special Issue: Biological Applications of Dendrimers

Received: November 3, 2011
Revised: December 10, 2011
Accepted: December 27, 2011
Published: December 29, 2011

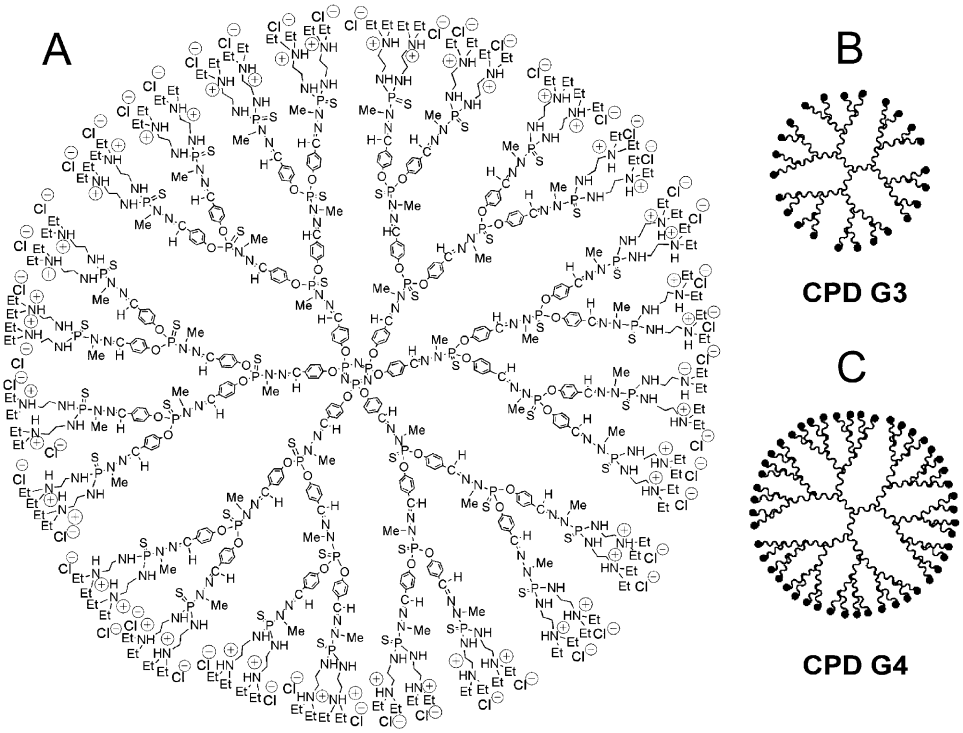

Figure 1. Developed structure of CPD generation 3 (A) and difference between generation 3 (B) and generation 4 (C).[39]

microtubules, and that leads to the disruption of the cellular transport and death of neurons. Not only is the presence of intracellular MAP-Tau aggregates restricted to AD but they also appear in other neurodegenerative diseases called taupathies such as Pick's disease, corticobasal degeneration and progressive supernuclear palsy.[20−22]

Since one of the main molecular causes of neurodegenerative diseases is the accumulation of misfolded and aggregated protein, attempts to cure the diseases concentrate on blocking or reversing the protein conformational and aggregational changes and diminishing the neurotoxic forms.[23]

Dendrimers are a relatively new group of polymers. All dendrimers are built from a central core molecule, which is surrounded by layers of branched monomers. Each layer of monomers defines a so-called generation of dendrimers. As a result, the dendrimers adopt a globular shape with a densely packed surface. Dendrimers are being extensively studied for their potentially important applications in biotechnology and medicine e.g. as nonviral vectors or drug transporters.[24−28] Cationic dendrimers enter the cell by electrostatic interaction and/or by nonspecific absorptive fluid-phase endocytosis.[29−31] It is known that dendrimers have high affinity toward proteins and can affect amyloidogenesis by inhibiting or accelerating production of fibrils.[28,32,33] Moreover poly(aminoamide) (PAMAM) and poly(propyleneimine) (PPI) dendrimers are able to purge scrapie forms of prion protein from infected brains.[34−36]

In the present work, we have focused on comparing the impact of two generations (3 and 4) of phosphorus dendrimers (CPDs) on amyloid fibril formation and the MAP-Tau aggregation process. Previously interactions between phosphorus dendrimers and prion peptide $PrP_{185−208}$ were studied.[37] However, up to now, it has not been checked whether these dendrimers have an influence on processes that are characteristic for Alzheimer's disease.

EXPERIMENTAL SECTION

Materials. Synthetic peptide $A\beta_{1−28}$ [DAEFRHDSGYEVHHQKLVFFAEDVGSNK] was purchased from JPT Peptide Technology (Germany). Peptide stock solution was kept in aqueous 10 mM HEPES buffer at neutral pH. Thioflavin T (ThT) (T-3516) was purchased from Sigma Chemical Company and dissolved to a concentration of 8 mM in 10 mM HEPES pH 7.4. Heparin-sodium salt (H-4784) was purchased from Sigma Chemical Company and dissolved to 15 mg/mL in 10 mM HEPES pH 7.4.

Cationic phosphorus dendrimers (CPDs) were synthesized in the Laboratoire de Chimie de Coordination du CNRS. They are characterized by the presence of aminothiophosphates at each branching point which may enhance their biocompatibility.[38−41] The schematic structure of dendrimers is presented in Figure 1, and the main characteristics are gathered in Table 1.

Table 1. Main Characteristics of CPDs

	CPD G3	CPD G4
generation	3	4
chem composition	$C_{624}H_{1104}N_{183}C_{148}O_{42}P_{45}S_{42}$	$C_{1296}H_{2256}N_{375}C_{96}O_{90}P_{93}S_{90}$
surf cationic end groups	48	96
mol wt [Da]	16,280	33,702
diam [nm]	4.1	5.0

All other used reagents were of analytical grade and purchased from Sigma-Aldrich Chemical Co. Water used to prepare solutions was Milli-Q.

MAP-Tau Purification. Plasmid pET29b encoding human Tau (2N4R) described by Hedgepeth and colleagues[42] was purchased from Addgene (Cambridge, MA, USA). To obtain His_6-tagged protein, Tau coding sequence was cloned into pET28a vector (Novagen, Madison, WI, USA). The *Escherichia coli*

dx.doi.org/10.1021/mp2005627 | *Mol. Pharmaceutics* 2012, 9, 458−469

BL21 (DE3) cells transformed with Tau/pET28a were collected by centrifugation at 6000*g* for 10 min. Bacterial pellets were resuspended in column buffer composed of 500 mM NaCl, 19 mM β-ME, 1 mM PMSF and 50 mM sodium phosphate pH 7.0, by four cycles of sonication (30 s each, S250D sonifier, Branson Ultrasonics, Danbury, CT, USA). The supernatant obtained after centrifugation for 20 min at 21000*g*, 4 °C, was boiled for 10 min in water bath and after cooling centrifuged for 1.5 h at 100000*g*, 4 °C. The resultant supernatant was filtered through a 0.45 μm syringe filter (Millipore, Billerica, MA, USA) and loaded on Ni-NTA resin (Qiagen, Valencia, CA, USA). The resin was washed with the column buffer and subsequently with the column buffer containing 20 mM imidazole (pH 7.0). Tau was eluted by the column buffer supplemented with 100 mM imidazole and salted out by ammonium sulfate at 50% saturation. The pellet of pure Tau obtained after centrifugation for 30 min at 40000*g*, 4 °C, was resuspended and dialyzed against 50 mM NaCl, 1 mM DTT, 1 mM PMSF and 50 mM MES pH 6.8. Protein concentration was determined by Bradford method,[43] and purity of preparations was assessed by SDS−PAGE.

Formation of Aβ_{1-28} Fibrils: ThT Assay. The aggregation process was monitored using thioflavin T (ThT). Fluorescence of ThT increases when it binds to β-sheet aggregate structures such as amyloid fibrils. Stock solution of Aβ_{1-28} peptide (1 mM) in HEPES buffer, pH 7.4, was diluted to a final concentration of 50 μM and subjected to sonication 5 times per 10 s using a UD-11 ultrasonic disintegrator (Techpan, Poland). ThT was added to a final concentration of 35 μM, and pH was adjusted to 5.5 with aliquots of HCl. The aggregation process was triggered by the addition of 0.041 mg/mL of heparin. CPDs were added at concentrations of 0.01 μM, 0.1 μM, 1 μM, and 10 μM in the beginning of the process. In other experiments CPDs at concentrations of 0.01 μM and 1 μM were added 25 min after addition of heparin. Fluorescence measurements were carried out with a Perkin-Elmer LS-50B spectrofluorimeter. Excitation and emission wavelengths were set at 450 and 490 nm, respectively. Temperature was controlled with a thermostatic bath at 37 °C.

Formation of MAP-Tau Aggregates: ThS Assay. Solution of MAP-Tau at a concentration of 0.4 mg/mL (3.87 μM) was prepared in 10 mM PBS (pH 7.4) supplemented with 2.5 mM DTT, 1 mM EDTA, 1 mM EGTA, 1 mM PMSF. CPDs were added in two different concentrations, 0.58 μM and 5.8 μM, that correspond to molar ratios CPD/MAP-Tau equaling 0.15 and 1.5, respectively. ThS was added to a final concentration of 35 μM. The aggregation process was triggered by the addition of 0.2 mg/mL of heparin. Fluorescence intensity was measured with Horiba Fluorolog 3. Excitation and emission wavelengths were set at 440 and 510 nm, respectively. Temperature was controlled with a thermostatic bath at 25 °C.

Cell Culturing. Mouse neuroblastoma (N2a) cell line (ATCC No. CCL-131) was used. Cells were cultured in Dulbecco's modified Eagle's medium Gluta-MAX (DMEM) (Gibco) containing 10% fetal bovine serum in an atmosphere of 5% CO_2. Medium was replaced every 3 to 4 days, and cells were split for subcultures 1:5 every 4 to 5 days.

Cytotoxicity: MTT Assay. MTT assay is a standard cytotoxicity assay that measures mitochondrial oxidoreductase enzyme activity.[44−46] N2a cells were seeded in 96-well microplates (Greiner, Germany) at a density of 5×10^3 cells/well in 100 μL of DMEM. To check cytotoxicity of CPDs and Aβ_{1-28} species during the aggregation process, 24 h after cell attachment, plates were washed with 100 μL/well PBS (150 mM NaCl, 2 mM, KH_2PO_4, 10 mM Na_2HPO_4, 2.7 mM KCl, pH 7.4) and the cells were treated with increasing concentrations of each generation of CPDs (5 μL) or samples containing an Aβ_{1-28}/CPD mixture (5 μL). The samples containing Aβ_{1-28} and CPDs were taken from the experiment where the formation of Aβ_{1-28} fibrils was monitored by ThT assay during the aggregation process at different times (from 0 to 180th minute). Cells were incubated at 37 °C in a 5% CO_2 humidified incubator. Five to six replicate wells were used for each control and test concentration. After 24 h of dendrimer or Aβ_{1-28}/dendrimer mixture exposure, the medium was removed, the cells were washed with PBS and 100 μL of freshly prepared MTT (0.5 mg/mL of MTT in PBS) was added to each well. After 4 h of incubation, the medium was discarded, the cells were rinsed with PBS, 100 μL of MTT fixative solution (DMSO) was added to each well, and plates were shaken for 5 min. The absorbance was measured at 540 nm (reference 720 nm) with a Cary 50 BIO UV−visible spectrophotometer. The viability was calculated as follows:

$$\text{viability}\,[\%] = (x/x_C) \times 100\%$$

where x is the absorbance of an investigated sample and x_C is the absorbance of a control (untreated) sample.

Circular Dichroism Experiments and Analysis. CD measurements in the far-UV region were carried out with a J-815 CD spectrometer (Jasco). All Aβ samples were sonicated 5 times under cooling conditions for 10 s using UD-11 ultrasonic disintegrator (Techpan, Poland). The concentration of the Aβ_{1-28} was 50 μM. CD spectra were registrated between 260 and 190 nm using 0.05 cm path length quartz sandwich cell (Helma). The recording parameters were as follows: bandwidth, 1.0 nm; slit width, auto; response, 1 s; scan speed, 50 nm/min; and step resolution, 0.2 nm. The number of scans varied between three and five for each sample. Measurements were done for different time intervals during the aggregation process (5 min, 60 min, 120 min, and 180 min, counting from the beginning of the process). Finally the CD spectra were corrected by subtracting CD spectra obtained for CPDs dissolved in a buffer without the peptide. The mean residue ellipticity θ,[47,48] expressed as a value deg cm^2 dmol^{-1}, was calculated. To estimate the secondary structure contents of the Aβ_{1-28} forms, an analysis of the relevant CD spectra was carried out using CDNN software.[49]

Transmission Electron Microscopy Observations of Aβ_{1-28}. Fifteen microliters of a sample was removed from a fluorimetric cuvette (see a ThT assay), placed on a copper grid with carbon surface for 10 min and dried with a filter paper. The sample was stained with 2% (m/v) uranyl acetate for 2 min and dried. Transmission electron microscopy images were performed using a Hitachi H-7000 (75 kV) microscope.

Transmission Electron Microscopy Observations of MAP-Tau. Recombinant MAP-Tau (human isoform 2N4R) at 7.5 μM was incubated in 5-fold diluted PBS, 1 mM EDTA, 1 mM EGTA, 1 mM PMSF, 2.5 mM DTT and heparin (Sigma, St. Louis, MO, USA) at 0.2 mg/mL for 72 h, at 25 °C. The incubation was carried out either with or without 5 μM CPD dendrimers. After 3 day incubation 10 μL samples were placed on 400-mesh copper grids (Sigma) covered with collodion (SPI Supplies, West Chester, PA, USA) and carbon. The samples were incubated for 40 s on the grids and drained with blotting paper. Subsequently, negative staining was performed with 2% (w/v) uranyl acetate (SPI Supplies) for 25 s. The grids were

examined at an accelerated voltage of 80 kV in a JEM 1400 electron microscope (JEOL Ltd., Tokyo, Japan) equipped with a digital camera (CCD MORADA, SiS-Olympus, Muenster, Germany).

Fluorescence Spectra of Tyrosine Residues in Aβ_{1-28}. Aβ_{1-28} possesses one tyrosine residue located in a position of 10 (Tyr^{10}). 100 μM stock solution of the peptide was dissolved in PBS (pH 7.4), to avoid aggregation of Aβ_{1-28}, and diluted to a concentration of 50 μM. Experiments were carried out with a Perkin-Elmer LS-50B spectrofluorometr using 1 cm quartz cells with continuous stirring. Samples were thermostated at 25 °C. One milliliter of Aβ_{1-28} was titrated with CPDs in a concentration range from 0.01 to 0.75 μM (stock solution of dendrimers was 200 μM in PBS). The excitation wavelength was 273 nm, and the emission spectra were recorded from 286 to 340 nm.

The Effect of CPDs on Fluorescence of Free L-Tyrosine. L-Tyrosine was dissolved at a concentration of 100 μM in PBS (pH 7.4) and diluted to a concentration of 50 μM. The excitation wavelength was set at 273 nm, and the emission spectra were recorded from 286 to 340 nm. CPDs were added at concentrations from 0.01 to 0.75.

Statistical Analysis. All experiments were conducted in at least three independent experiments. Statistical analysis was performed using one way analysis of variance (ANOVA) followed by *t*-Tukey's multiple comparison test. Statistical significance was accepted at $P \leq 0.05$ for all tests. Analysis was performed using Statistica 5.5 (Stat Soft Poland) software. Results were expressed as means ± standard deviation (SD).

RESULTS

Amyloid Fibril Formation. Fluorescence of ThT. Formation of fibrils was monitored using a fluorescent dye Thioflavin T in the presence of heparin (0.041 mg/mL) that at acidic pH triggers the aggregation process. Figure 2 illustrates how CPD G3 and CPD G4 affect Aβ_{1-28} peptide (50 μM) aggregation at pH 5.5, 37 °C. A control curve (the system without dendrimers) shows a typical Aβ_{1-28} aggregation process. Fibrils were steadily created, and a plateau was obtained after approximately 150 min. When CPDs were applied in a high enough concentration (1 μM and 10 μM), they completely inhibited the aggregation process. The lowest concentration of dendrimers (0.01 μM) caused acceleration of fibril formation. The final amount of fibrils was significantly higher than for a control, and a plateau was obtained after approximately 60 min. A difference in a behavior between CPD G3 and CPD G4 was observed for 0.1 μM concentration. In the case of CPD G3 this concentration caused almost no effect, but in the case of CPD G4 it accelerated the process of fibrilization.

CPDs acted similarly (in terms of accelerating or inhibiting the fibrillization) when they were added 25 min after the aggregation process had started. A low concentration accelerated the process, whereas a high concentration caused disruption of fibrils. ThT fluorescence intensity was as low as in the beginning of the process (Figure 3).

Transmission Electron Microscopy of Aβ_{1-28} Fibril Formation. The effect of CPDs on the morphology of Aβ_{1-28} amyloid aggregates was analyzed using transmission electron microscopy. Small samples were taken from the cuvette of the ThT experiment when the sample was fully aggregated (180 min after the aggregation process started). For control samples and for samples containing 0.01 μM dendrimers the characteristic long Aβ_{1-28} fibrils were observed which clearly are seen in

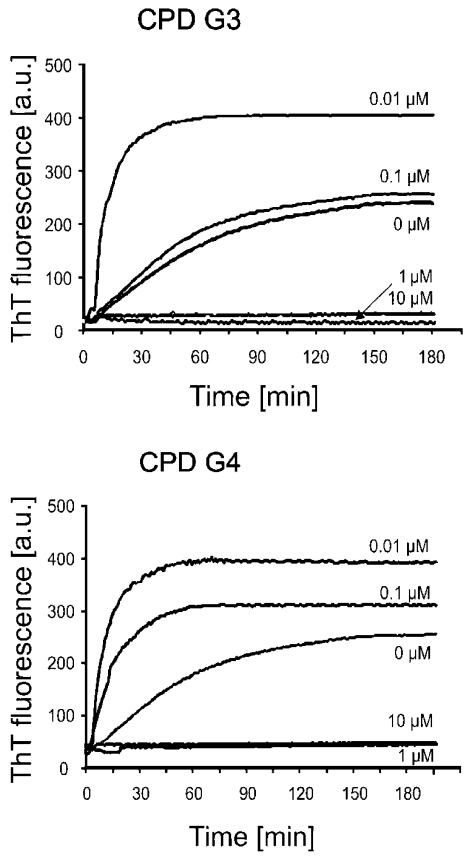

Figure 2. ThT fluorescence intensity during the aggregation process of the Aβ_{1-28} (50 μM) amyloid peptide in presence of CPD G3 and CPD G4.

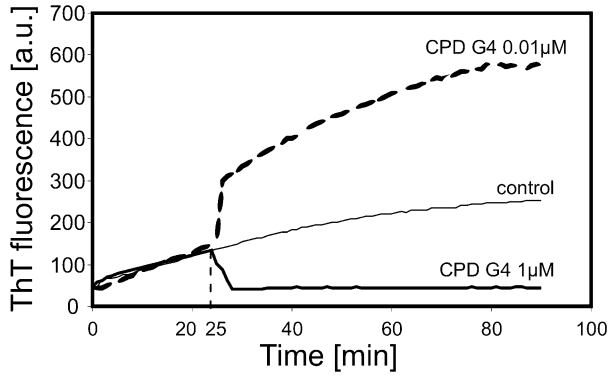

Figure 3. ThT fluorescence intensity during the aggregation process of the Aβ_{1-28} (50 μM) after addition of CPD G4 in the 25th minute of the process.

Figure 4 (the top and the middle panels respectively), whereas in the presence of the same dendrimers in a concentration of 10 μM the Aβ_{1-28} fibrils were not found (Figure 4 bottom panels).

CD Spectroscopy of Aβ_{1-28} Forms. To correlate the amount of created fibrils, observed by changes in ThT fluorescence intensity, with the variations in a secondary structure of Aβ_{1-28}, CD experiments were carried out on analogous samples that were used in the fluorescence experiments. Various concentrations of dendrimers (0.01 μM, 0.1 μM, 1 μM, and 10 μM) were added to Aβ_{1-28} (50 μM), and CD spectra were recorded at the following time intervals: 1 min, 60 min, 120 min, 180 min, and 240 min. CD spectra are

dx.doi.org/10.1021/mp2005627 | *Mol. Pharmaceutics* 2012, 9, 458−469

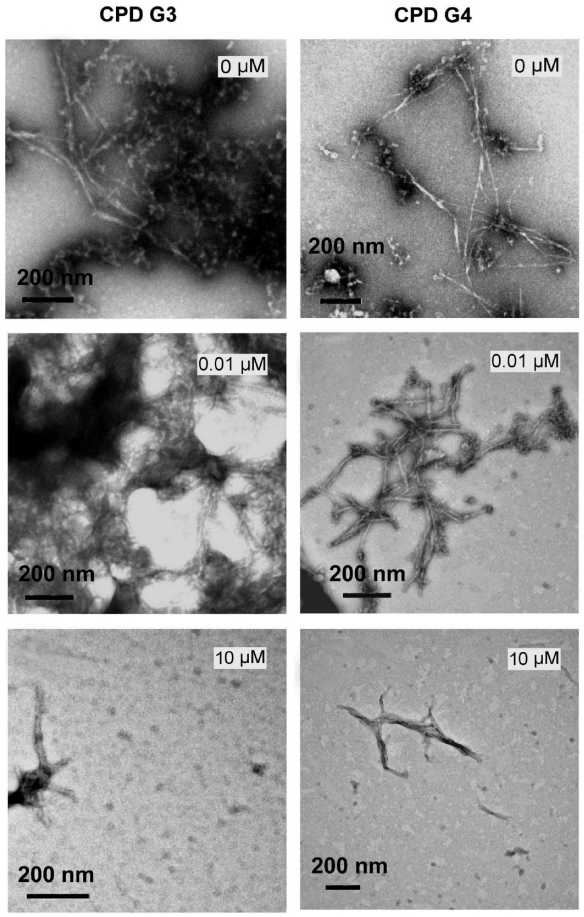

Figure 4. Electron micrographs of $A\beta_{1-28}$ samples at the end of the aggregation process without CPDs (top panels); in the presence of CPD G3 and CPD G4 at concentrations of 0.01 μM and 10 μM (middle and bottom panels, respectively). The length of the bar equals 200 nm.

displayed in the spectral region 190−260 nm (Figure 5). In this region the CD signal reflects the basic secondary structural features of peptides.[49−51] The spectrum obtained for non-aggregated $A\beta_{1-28}$ reveals a broad minimum between 195 and 210 nm. As the aggregation process developed, changes in the CD spectrum shape were observed. The most significant alterations were seen during the first hour. The next time intervals were not so significant. Upon addition of CPDs to $A\beta_{1-28}$ at concentrations that accelerated fibril formation (0.01 μM and 0.1 μM), spectra changed similarly to the control, whereas when CPDs completely inhibited fibril formation (for concentrations 1 μM and 10 μM), no changes in spectrum shape were observed.

CDNN software was used to analyze the CD spectra and monitor changes in a secondary structure. During the aggregation process the amount of α-helical and random structures gradually decreased and β-sheet structures increased in the system without CPDs (Table 2). When CPDs were applied in concentrations that inhibited fibril formation (1 μM and 10 μM), the composition of the secondary structure remained unchanged during the experiment time, whereas adding CPDs in lower concentrations (0.01 μM and 0.1 μM) caused faster and more pronounced conversion from a mixture of α-helical and random structures to β-sheet structures.

Formation of MAP-Tau Aggregates. Fluorescence of ThS. Aggregation of MAP-Tau protein was checked in a neutral buffer (10 mM PBS, pH 7.4) using a fluorescence dye thioflavin S. Fluorescence intensity of ThS was recorded for 66 h (Figure 6). A characteristic sigmoidal increase of ThS fluorescence intensity was observed for a control. A very similar behavior was observed when CPDs were added to the system in a molar ratio CPD/MAP-Tau equal to 0.15. However, when CPD concentration was ten times higher, both dendrimers significantly inhibited the aggregation process.

Transmission Electron Microscopy. Formation of MAP-Tau Aggregates. As it is demonstrated in electron micrographs (Figure 7A), during 3 day incubation with heparin, MAP-Tau formed numerous fibrillar structures corresponding to previously reported straight filaments, twisted filaments and paired helical filaments.[52] At these conditions granular Tau structures were rarely observed. Interestingly, dendrimers of both generations (CPD G3 and CPD G4), applied at the molar ratio to Tau of approximately 0.67, induced robust formation of granular structures assembling into large amorphous aggregates (Figure 7B,C). In the presence of CPD G3, this was accompanied by reduction of the number and length of Tau fibrillar aggregates (Figure 7B). At the same time, CPD G4 had less apparent effect on filamentous aggregation, however we observed some shortening of fibrillar structures (Figure 7C).

Cytotoxicity Experiments. MTT Assay. *Cytotoxicity of Dendrimers.* Figure 8 shows the effect of 24 h exposure of CPD G3 and CPD G4 on N2a cell line viability. Initially it was planned to check the same concentrations that were applied in previous assays. However, the effect of CPDs was too strong to test them at a concentration of 10 μM. Therefore, CPDs were tested in a concentration range from 0.025 μM to 3 μM. IC_{50} value (corresponding to 50% cell growth inhibition) equaled approximately 1 μM for both dendrimers.

Effect of Dendrimers on $A\beta_{1-28}$ Cytotoxicity. During the aggregation process of $A\beta_{1-28}$ the samples were collected and incubated with N2a cells. For a control (the system without CPDs) the samples were collected every 15 min until the 150th minute of the process and then after 30 min (the 180th minute of the process) (Figure 9, top panels). Time "zero" corresponds to the viability of cells that were not treated with the peptide. In the beginning of the process there were mainly nontoxic $A\beta_{1-28}$ monomers (the 15th minute). However, at the 30th minute the toxicity was much more pronounced, and the maximal toxic effect was observed after 60 min. Since then the toxicity was gradually reduced unless it reached a plateau value (viability equal to approximately 80%) for the 135th minute. In the cases when CPDs significantly accelerated the fibril formation, there was a need to apply shorter time intervals (every 5 min). The minimal cell viability was reached in the 10th or 15th minutes. It is worth noticing that nevertheless the minimal value was significantly higher than for the control (50−60% compared to approximately 30%). Afterward the cytotoxicity decreased, reaching a plateau value in the 40th minute for CPDs at a concentration of 0.01 μM. When CPDs inhibited fibril formation at a concentration of 1 μM, cell viability gradually decreased from values of approximately 100% to approximately 80% reached after 90 min. A similar behavior was observed when CPDs were added in a concentration of 10 μM with only one difference—the final value of cell viability was lower—75% to 65%.

Tyrosine Quenching Experiments. Intrinsic peptide fluorescence is a useful and sensitive tool to study variations

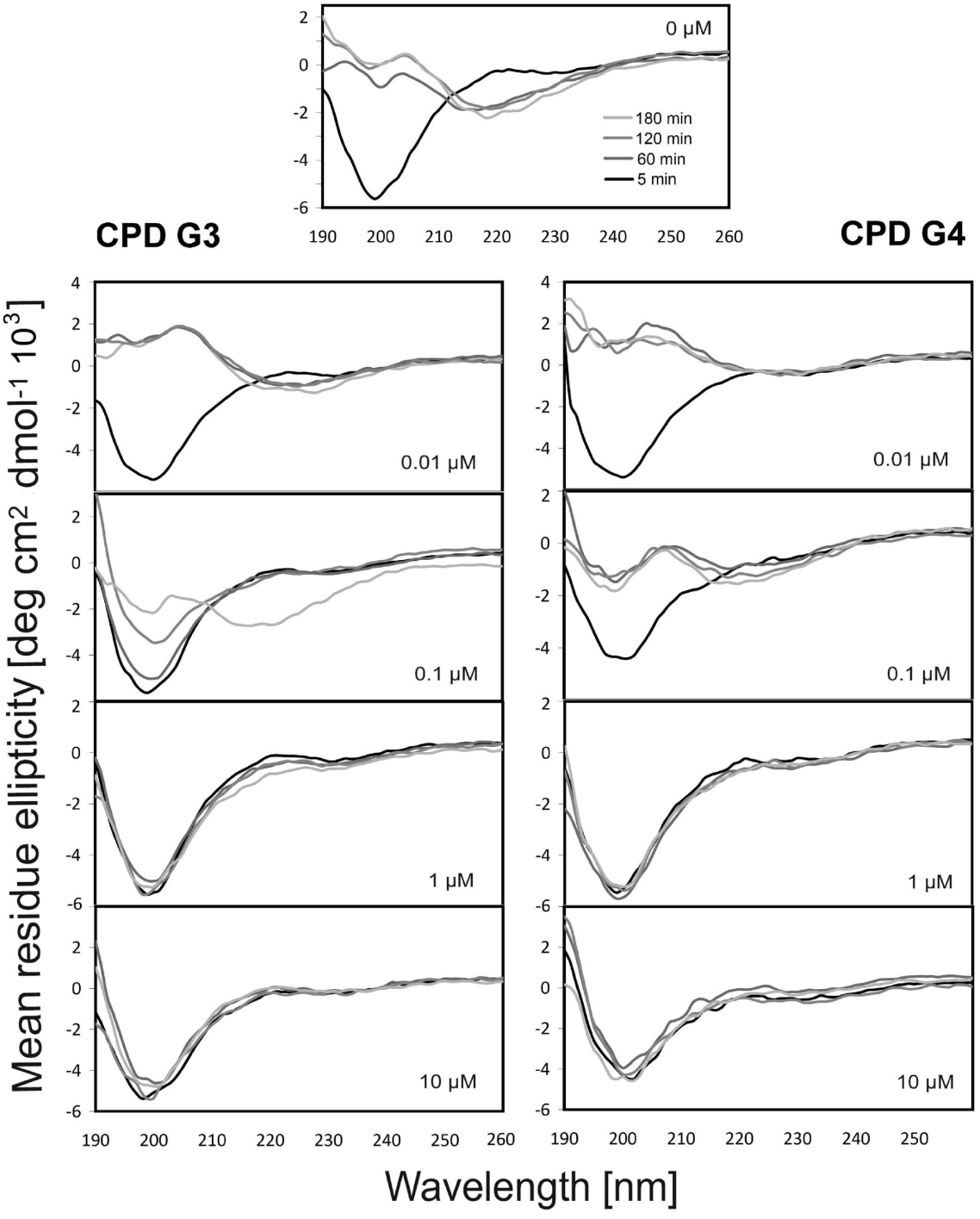

Figure 5. CD spectra of Aβ_{1-28} during the aggregation process without CPDs (top) and with CPD G3 (left panels) and CPD G4 (right panels).

in a peptide conformation and its interactions with other molecules. Aβ_{1-28} possesses one tyrosine residue that emits fluorescence with the maximum at 304 nm upon excitation at 273 nm. The decrease in the fluorescence intensity was the most marked change upon successive addition of CPD G3 and CPD G4 in 10 mM PBS, pH 7.4, indicating that dendrimers quench the fluorescence of Aβ_{1-28} (Figure 10A,B). A very similar quenching effect was observed for the system free L-tyrosine and CPDs (Figure 10C,D). However, in the case of a free amino acid no shift of emission spectra was observed, whereas for a tyrosine residue in Aβ_{1-28} such a shift upon addition of CPDs was apparent. Therefore this parameter was analyzed. The shift in a position of emission maximum is correlated with changes in polarity around the chromophore. The red shift indicates that fluorophore is more exposed to the solvent, whereas the blue shift is related with burying fluorophore into a more hydrophobic environment.[53] We registered a ratio of fluorescence intensity at two wavelengths, on the left (F_L, 298 nm) and on the right (F_R, 310 nm) slopes of the spectrum (Figure 11). Figure 12 shows the effect of CPDs on a position of emission maximum. A red shift was observed for both dendrimers, but it was bigger after addition of CPD G4.

dx.doi.org/10.1021/mp2005627 | *Mol. Pharmaceutics* 2012, 9, 458−469

Table 2. The Percentage (±3%) of Secondary Structures of Aβ 1-28[a]

	CPD G3 [%]					CPD G4 [%]				
dendrimer concn [μM]	1[b]	60	120	180	240	1	60	120	180	240
					α-Helix					
0	30.0	28.5	26.4	22.9	22.2	30.0	28.5	26.4	22.9	22.2
0.01	29.1	18.3	18.3	17.9	15.9	29.1	17.7	17.7	16.9	16.9
0.1	28.4	26.7	19.4	16.8	16.8	27.5	24.2	22.1	22.9	20.0
1	28.0	28.1	27.8	26.7	25.6	27.6	27.1	26.7	26.1	28.1
10	28.0	27.9	27.7	27.3	28.2	25.9	26.0	26.0	25.9	25.8
					β-Stuctures					
0	40.0	47.5	51.7	55.2	54.8	40.0	47.5	51.7	55.2	54.8
0.01	36.5	52.7	52.4	52.4	57.2	36.5	54.4	54.2	54.0	54.9
0.1	33.6	40.6	49.9	58.3	58.7	42.1	49.3	51.0	52.1	58.0
1	41.0	40.2	40.1	40.0	40.5	42.0	42.2	42.5	42.5	42.1
10	39.2	39.3	39.5	39.9	40.2	43.5	43.5	43.4	43.5	43.5
					Random Coil					
0	30.0	24.0	21.9	21.9	23.0	30.0	24.0	21.9	21.9	23.0
0.01	34.4	29.0	29.3	29.7	26.9	34.4	29.0	29.1	29.3	29.2
0.1	38.0	32.7	30.7	24.9	24.5	30.4	26.5	24.9	25.0	22.0
1	31.1	32.1	32.4	34.1	34.5	30.4	30.8	31.1	31.5	30.2
10	33.1	33.2	33.4	33.6	33.1	31.5	31.5	31.5	31.5	31.6

[a]CD spectra presented in Figure 5 were deconvoluted with CDNN software (see Experimental Section for details). [b]Time of aggregation [min].

DISCUSSION

Formation of amyloid plaques in the brain is one of the major pathological hallmarks of AD. β-Amyloid peptide consisting of 40−42 amino acid residues (Aβ 1−40, Aβ 1−42) is the main component of amyloid deposits. Aβ has a high tendency to aggregate by forming oligomers, protofibrils, and fibrils. Therefore, clearing of Aβ from the brain and preventing aggregation of Aβ are two actively pursued therapeutic strategies for treating AD. CPDs have never been tested in the context of AD, even though several other types of dendrimers such as polyamidoamine (PAMAM) and polypropyleneimine (PPI) dendrimers have revealed some interesting properties.[28,33,36] Moreover, it has been proven that CPDs are able to purge prion protein PrP^{Sc} from infected cells[38] similarly to PAMAM dendrimers.[34] This fact was an inspiration to check the influence of CPD G4 on fibril formation from prion peptide PrP 185−208.[37] A structural homology has been described for the segment of prion protein PrP 185−208 and Alzheimer's peptide Aβ 1−28 identified as a possible binding domain.[54] Therefore, in the present studies Aβ 1−28 has been chosen as a model Alzheimer's peptide. The influence of CPDs on the process of creating fibrils was checked using ThT as a fluorescent probe. The concentration of Aβ 1−28 (50 μM) and the conditions (adding heparin at a concentration of 0.041 mg/mL, lowering pH to 5.5) were exactly the same as in previous experiments performed for PAMAM and PPI dendrimers[28,33,36] to be able to compare CPDs to other dendrimers. As most previously tested dendrimers, CPDs blocked fibril formation when used at high concentrations, whereas they accelerated the production of fibrils at lower concentrations. This finding was further confirmed by transmission electron microscopy observations. For low and high concentrations both generations (CPD G3 and CPD G4) behaved similarly, whereas different behavior was noticed for a concentration equal to 0.1 μM. It shows that the size of the dendrimer and the number of terminal groups play an important role. Different behavior seen for low and high concentrations is a typical pattern for fibril disrupting agents. Inhibitors that increase a fibril breakage rate, when administerated in low doses, can accelerate fibrillogenesis by providing a larger amount of fibril ends that serve as sites of replication. However, in higher doses breakage is very fast and fibrils break down. This hypothesis can be also drawn based on a different experimental system when CPD G4 at a concentration of 1 μM was added 25 min after starting the aggregation process. Fluorescence intensity of ThT decreased to the same level as for CPD G4 (at a concentration of 1 μM) applied in the beginning of the process. It means that CPD G4 was able to disrupt fibrils that had been preformed. It is known that creation of fibrils is accompanied by changes in a peptide secondary structure because β-forms are characteristic for aggregates. Therefore, we have used circular dichroism spectroscopy (CD) to monitor these changes over the aggregation process. Conditions and concentrations were exactly the same as in the ThT assay. For a control (nonaggregated Aβ 1−28 without CPDs), the content of α-helical, random, and β-structures was 30%, 30%, and 40%, respectively. Over time, as the aggregation process progressed, the amount of β-structures increased, whereas the percentage of the rest of the structures decreased, reaching at the end the following final values: α-helix, 22%; random coil, 23%; and β-structures, 55%. Results obtained for systems with CPDs confirmed earlier observations. Low concentrations of CPDs caused a faster and more pronounced conversion to β-sheets. CD spectra remained unchanged when high concentrations of CPDs were applied. This finding means more than just a confirmation of results received from a ThT assay. The ThT assay allows the monitoring of production of fibrils. The lack of changes in a secondary structure, observed upon addition of CPDs at high concentrations, indicates that no oligomers were created because oligomers predominantly consist of β-structures. Therefore CD experiments showed that CPDs at high concentrations not only block fibril formation but also prevent production of oligomers. This can happen due to interactions between CPDs and monomeric forms of Aβ 1−28. Such a hypothesis can be drawn based on changes in intrinsic fluorescence of Aβ 1−28 upon addition of CPDs.

dx.doi.org/10.1021/mp2005627 | Mol. Pharmaceutics 2012, 9, 458−469

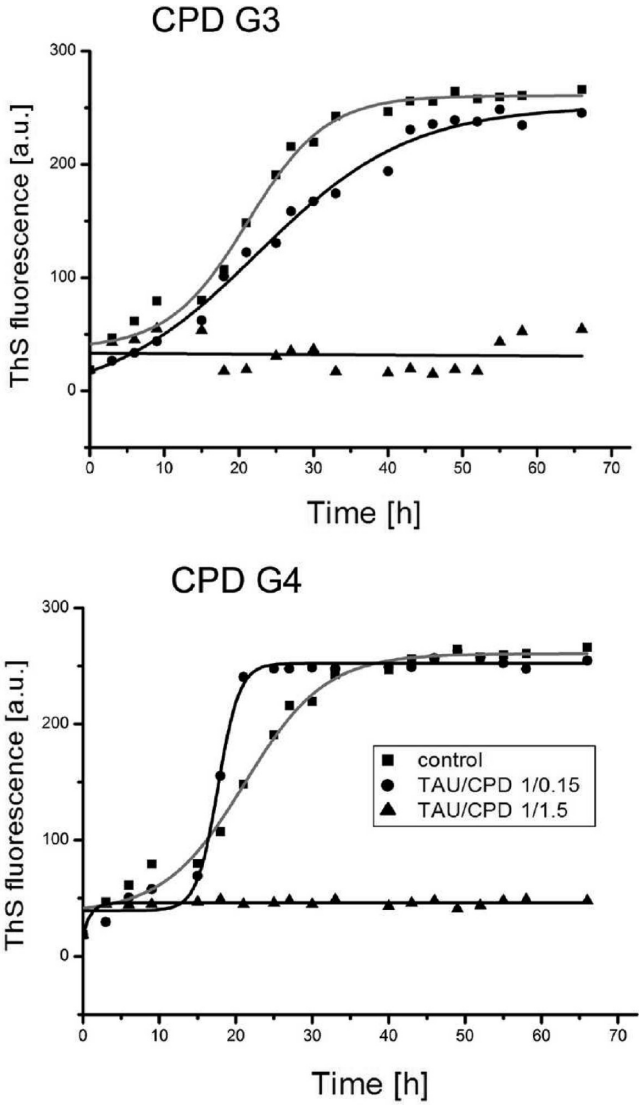

Figure 6. ThS fluorescence intensity during the aggregation process of MAP-Tau protein in the presence of CPDs.

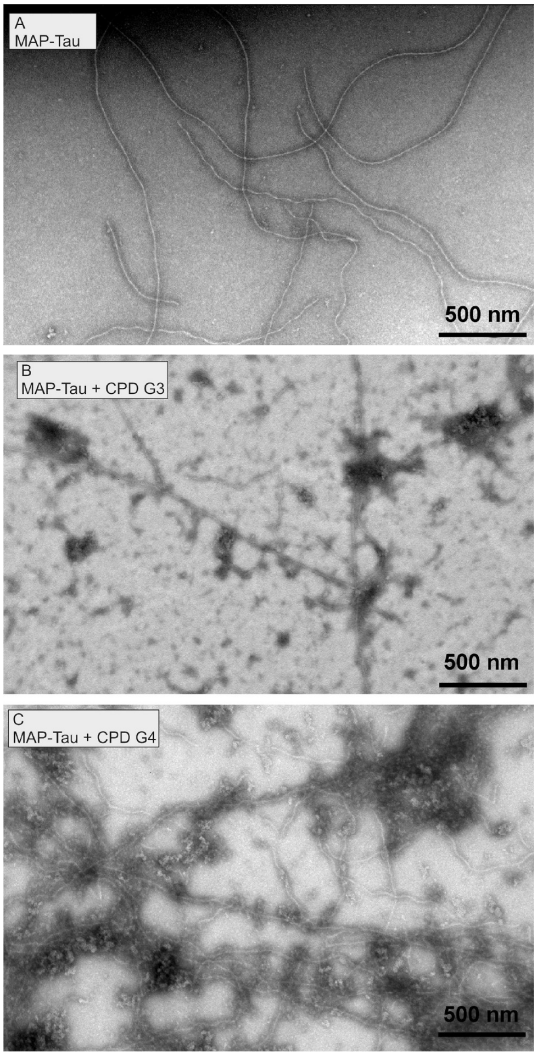

Figure 7. Electron micrographs of MAP-Tau samples. In the absence of CPDs, Tau formed predominantly fibrillar structures (A). Tau incubated with CPD G3 and CPD G4 at the molar ratio of 1.5:1 assembled into numerous amorphous aggregates (B, C). In the presence of CPD G3 this amorphous aggregation was accompanied by substantial reduction in the formation of fibrillar structures (B), whereas CPD G4 had a moderate effect on Tau filamentous aggregation (C).

These experiments were performed in neutral pH to avoid the aggregation process and ensure that the observed effect was due to interactions between CPDs and monomeric forms of Aβ 1−28.

Cytotoxicity of nonaggregated and aggregated forms of Aβ 1−28 was checked during the aggregation process by an MTT assay. In the beginning no toxic effect was found, but as oligomerization was progressing the system was becoming more and more toxic until minimal cell viability was reached. Then the toxicity was gradually diminished. This observation is consistent with recent findings saying that fibril intermediates such as oligomers and protofibrils are more toxic than mature fibrils.[55] When CPDs were present in the system in concentrations of 1 μM and 10 μM, a slight toxic effect was observed since the 90th minute. It can be a consequence of the presence of a certain aggregated form (visible at TEM pictures) or comes from CPDs which demonstrated strong toxicity in this concentration range. It is worth noting that no additive effect was observed. On the contrary, the toxicity of CPDs themselves was much bigger than when they were in the system with Aβ 1−28. It means that interactions between CPDs and Aβ 1−28 not only stopped the harmful oligomerization processes but also diminished toxicity of CPDs. Toxicity of

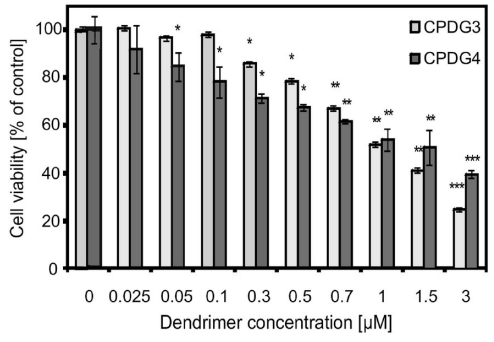

Figure 8. Effect of increasing concentrations of CPD G3 or CPD G4 on mouse neuroblastoma cell (N2a) viability (* $p < 0.05$, ** $p < 0.01$. *** $p < 0.005$).

cationic dendrimers is mainly a result of their interactions with negatively charged membranes. Aβ 1−28 is an acidic peptide;

dx.doi.org/10.1021/mp2005627 | *Mol. Pharmaceutics* 2012, 9, 458−469

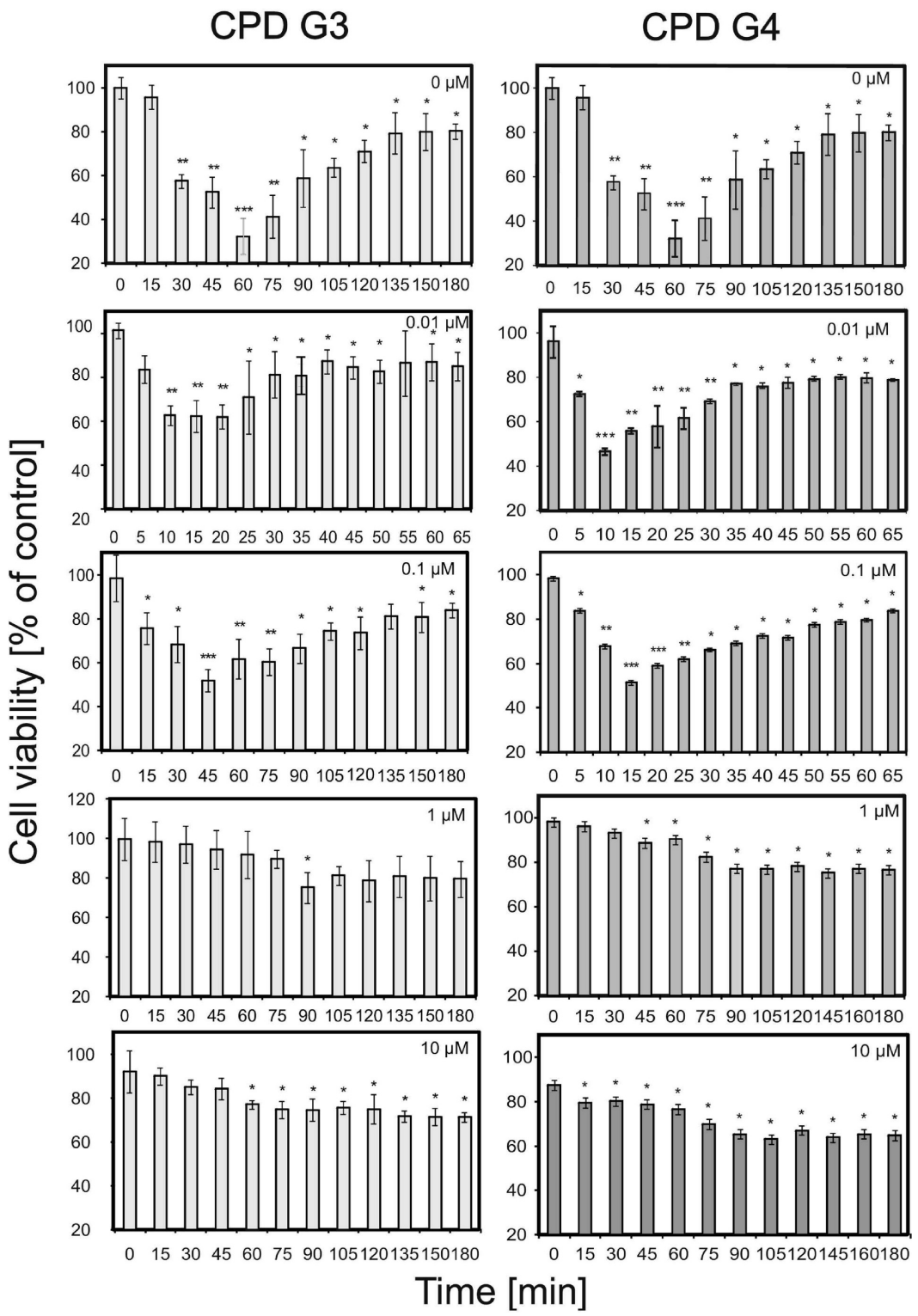

Figure 9. Effect of $A\beta_{1-28}$ forms (at different aggregation stages) on mouse neuroblastoma cell line viability in the presence of CPDs (* $p < 0.05$, ** $p < 0.01$. *** $p < 0.005$).

therefore these dendrimers that electrostatically interacted with the peptide became less harmful to negatively charged cell components, because the amount of accessible cationic groups on the dendrimer's surface decreased. A different influence of CPDs on toxicity of Aβ 1−28 forms was observed when CPDs were added to the system in concentrations that accelerated fibril formation (0.01 μM and 0.1 μM). In this case the toxicity came only from Aβ 1−28 because low concentrations of CPDs (especially 0.01 μM) were not toxic. In the presence of CPDs as fibrillization progressed a similar effect was observed as for the control (reaching the minimum of cell viability and afterward cell viability gradually increased). However, compared to the control, there were two important differences: the minimal values of cell viability were significantly higher, and the

dx.doi.org/10.1021/mp2005627 | *Mol. Pharmaceutics* 2012, 9, 458−469

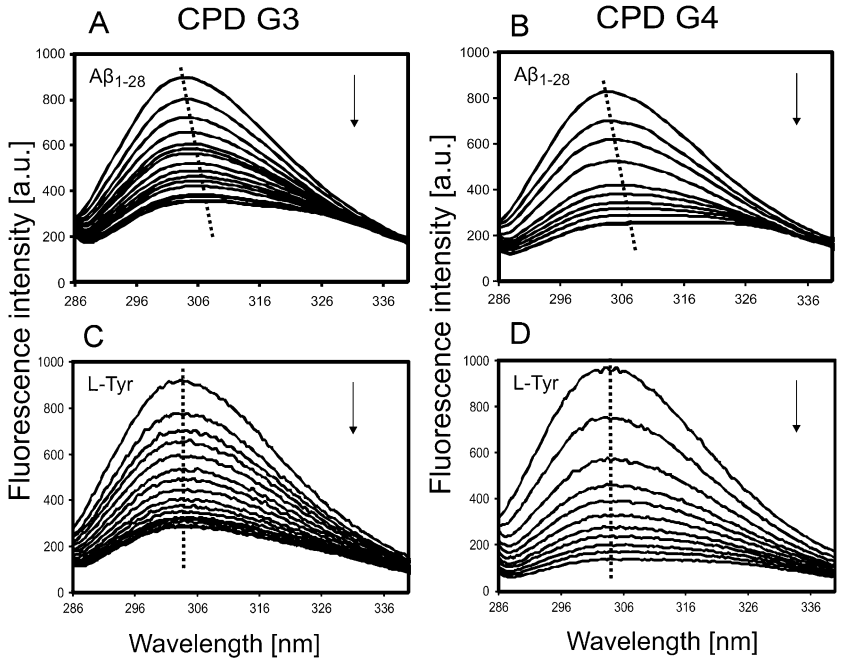

Figure 10. Fluorescence spectra of Aβ_{1-28} in the absence (top line) and presence of CPD G3 (from 0.05 to 0.75 μM), left panel, and CPD G4 (from 0.05 to 0.5 μM), right panel. Arrows indicate the progress of titration.

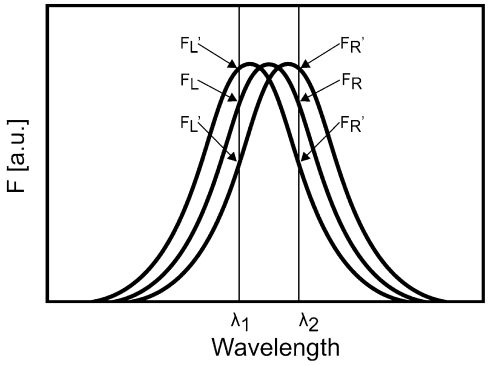

Figure 11. The scheme of the double-wavelength method to calculate the position of emission maximum.

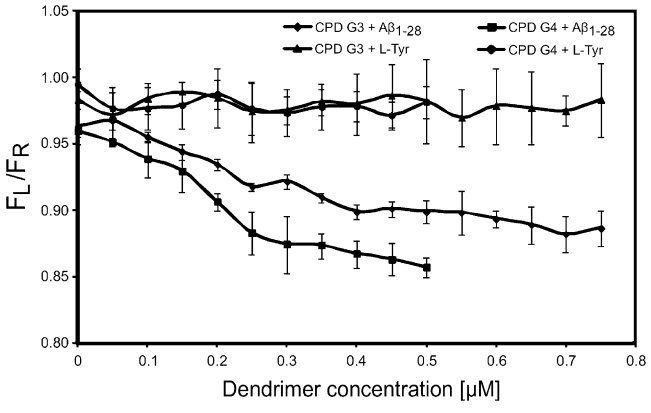

Figure 12. Effect of CPDs on emission maximum registered as a ratio of fluorescence intensity at two wavelengths: on the left (F_L) and on the right (F_R) slope of the spectrum.

period when the system was severely toxic (cell viability below 60%) decreased from approximately 60 min for the control to approximately 15 min for the systems with CPDs.

Encouraged by promising results obtained for Aβ 1−28, we have decided to check whether CPDs have an influence on the aggregation of MAP-Tau protein. MAP-Tau is a microtubule-stabilizing protein whose aggregation, observed in Alzheimer disease (AD) and related taupathies, leads to loss of its function and neurodegeneration.[56] The microtubule associated MAP-Tau protein shows a tendency to assemble, dissociate from microtubules and form insoluble paired helical filaments (PHF). Filamentous aggregates of Tau—a hallmark of AD—are considered resultants of Tau hyperphosphorylation. The *in vitro* effect of this modification is mimicked by polyanionic cofactors like heparin and heparan sulfate.[52,57] In this study we have demonstrated for the first time the effect of dendrimers on Tau aggregation. In our experiments the CPDs' impact on aggregation behaviors of MAP-Tau was investigated using a fluorescent dye, ThS. It was shown that a 1:1.5 molar ratio of CPDs:MAP-Tau was effective in prevention of MAP-Tau amyloidogenesis. The effect of CPDs when their concentration was ten times lower was weak, and the ThS fluorescence intensity values were similar to the values for control samples not treated with CPDs. Using TEM we have found that CPDs induce aggregation of Tau into amorphous rather than filamentous structures. This amorphous aggregation may result from incubation of basic protein (p*I* calculated for Tau 2N4R is 8.24) with cationic dendrimers, whereas fibrillar aggregation is amply documented for Tau incubated with polyanionic molecules. It is postulated that soluble oligomers of hyperphosphorylated Tau rather than fibrillar aggregates are the most neurotoxic assemblies of Tau in AD.[56] Whether the dendrimer-induced amorphous aggregates of Tau described here are similarly nontoxic remains to be established.

To conclude, we have demonstrated that CPDs have an influence on two important factors in pathogenesis of Alzheimer's disease: they modify the aggregation of both amyloid peptide Aβ 1−28 and MAP-Tau protein. Moreover, CPDs reduce toxicity caused by aggregated forms of Aβ 1−28.

dx.doi.org/10.1021/mp2005627 | *Mol. Pharmaceutics* 2012, 9, 458−469

Therefore, CPDs are promising polymers as therapeutics for Alzheimer's disease.

AUTHOR INFORMATION

Corresponding Author

*Department of General Biophysics, University of Lodz, 141/143 Pomorska St., Lodz 90-236, Poland. Phone: +48 42 635 4429. Fax: +48 42 635 4474. E-mail: aklajn@biol.uni.lodz.pl.

ACKNOWLEDGMENTS

Studies were funded by project "Biological Properties and Biomedical Applications of Dendrimers" operated within Foundation for Polish Science TEAM programme cofinanced by the European Regional Development Found. Plasmid encoding Tau was provided as a generous gift from Prof. Peter S. Klein through the Addgene plasmid depository (Addgene plasmid 16316). Microscopic studies were performed in the Laboratory of Electron Microscopy (Nencki Institute of Experimental Biology, Warsaw, Poland) using equipment installed within the project sponsored by the EU Structural Funds: Centre of Advanced Technology BIM - Equipment purchase for the Laboratory of Biological and Medical Imaging.

ABBREVIATIONS USED

Aβ, β-amyloid peptide; AD, Alzheimer's disease; CD, circular dichroism; CPDs, cationic phosphorus dendrimers; G3, generation 3; G4, generation 4; Hep, heparin-sodium salt; MAP-Tau, microtubule-associated protein Tau; MTT, 3-(4,5-dimethylthiazol-2-yl)-2,5-diphenyltetrazolium bromide; TEM, transmission electron microscopy; ThT, thioflavin T; ThS, thioflavin S

REFERENCES

(1) Robert, J. C.; Lansbury, P. T. Amyloid fibrillogenesis: themes and variations. *Curr. Opin. Struct. Biol.* **2000**, *10*, 60−68.

(2) Dobson, C. M. The structural basis of protein folding and its links with human disease. *Philos. Trans. R. Soc.* **2001**, *356*, 133−145.

(3) Bucciantini, M.; Giannoni, E.; Chiti, F.; Baroni, F.; Formigli, L.; Zurdo, J. S. Inherent toxicity of aggregates implies a common mechanism for protein misfolding diseases. *Nature* **2002**, *416*, 507−511.

(4) Caughey, B.; Lansbury, P. T. Protofibrils, pores, fibrils, and neurodegeneration: separating the responsible protein aggregates from the innocent bystanders. *Annu. Rev. Neurosci.* **2003**, *26*, 267−298.

(5) Klein, W. L.; Stine, W. B. Jr; Teplow, D. B. Small assemblies of unmodified amyloid beta-protein are the proximate neurotoxin in Alzheimer's disease. *Neurobiol. Aging* **2004**, *25*, 569−580.

(6) Stefani, M.; Dobson, C. M. Protein aggregation and aggregate toxicity: new insights into protein folding, misfolding diseases and biological evolution. *J. Mol. Med.* **2003**, *81*, 678−699.

(7) Walsh, D. M.; Selkoe, D. J. Oligomers on the brain: the emerging role of soluble protein aggregates in neurodegeneration. *Protein Pept. Lett.* **2004**, *11*, 213−228.

(8) Wenk, G. L. Neuropathologic changes in Alzheimer's disease. *J. Clin. Psychiatry* **2003**, *9*, 7−10.

(9) Mirra, S. S.; Heyman, A.; McKeel, D.; Sumi, S. M.; Crain, B. J.; Brownlee, L. M.; Vogel, F. S.; Hughes, J. P.; van Belle, G.; Berg, L. The Consortium to Establish a Registry for Alzheimer's Disease (CERAD). Part II. Standardization of the neuropathologic assessment of Alzheimer's disease. *Neurology* **1991**, *41*, 479−486.

(10) Shoji, M.; Golde, T. E.; Ghiso, J.; Cheung, T. T.; Estus, S.; Shaffer, L. M.; Cai, X. D.; McKay, D. M.; Tintner, R.; Frangione, B. Production of the Alzheimer amyloid beta protein by normal proteolytic processing. *Science* **1992**, *258*, 126−129.

(11) Reddy, P. H.; Beal, M. F. Amyloid beta, mitochondrial dysfunction and synaptic damage: implications for cognitive decline in aging and Alzheimer's disease. *Trends Mol. Med.* **2008**, *14*, 45−53.

(12) Gouras, G. K.; Tsai, J.; Naslund, J.; Vincent, B.; Edgar, M.; Checler, F.; Greenfield, J. P.; Haroutunian, V.; Buxbaum, J. D.; Xu, H.; Greengard, P.; Relkin, N. R. Intraneuronal Aß42 Accumulation in human brain. *Am. J. Pathol.* **2000**, *156*, 15−20.

(13) Shibata, M.; Yamada, S.; Kumar, S. R.; Calero, M.; Bading, J.; Frangione, B.; Holtzman, D. M.; Miller, C. A.; Strickland, D. K.; Ghiso, J.; Zlokovic, B. V. Clearance of Alzheimer's amyloid β(1−40)-peptide from brain by LDL receptor-related protein-1 at the blood-brain barrier. *J. Clin. Invest.* **2000**, *106*, 1489−1499.

(14) Casserly, I.; Topol, E. Convergence of atherosclerosis and Alzheimer's disease: inflammation, cholesterol, and misfolded proteins. *Lancet* **2004**, *363*, 1139−1146.

(15) Colell, A.; Fernández, A.; Fernández-Checa, J. C. Mitochondria, cholesterol and amyloid beta peptide: a dangerous trio in Alzheimer disease. *J. Bioenerg. Biomembr.* **2009**, *41*, 417−423.

(16) Abramov, A. Y.; Fraley, C.; Diao, C. T.; Winkfein, R.; Colicos, M. A.; Duchen, M. R.; French, R. J.; Pavlo, E. Targeted polyphosphatase expression alters mitochondrial metabolism and inhibits calcium-dependent cell death. *Proc. Natl. Acad. Sci. U.S.A.* **2007**, *104*, 18091−18096.

(17) Bezprozvanny, I.; Mattso, M. P. Neuronal calcium mishandlingand the pathogenesis of Alzheimer's disease. *Trends Neurosci.* **2008**, *31*, 454−463.

(18) Fredhoff, A.; Schneider, A.; Mandelkow, E. M.; Mendelkow, E. Rapid assembly of Alzheimer-like paired helical filaments from microtubule-associated protein tau monitored by fluorescence in solution. *Biochemistry* **1998**, *37*, 10223−10230.

(19) Buee, L.; Busierre, T.; Buee-Scherrer, V.; Delacourte, A.; Hof, P. L. Tau protein isoforms, phosphorylation and role in neurodegenerative disorders. *Brain Res. Brain. Res. Rev.* **2000**, *33*, 95−130.

(20) Lee, V. M. Y.; Goedert, M.; Trojanowski, J. Q. Neurodegenerative tauopathies. *Annu. Rev. Neurosci.* **2001**, *24*, 1121−1159.

(21) Forman, M. S.; Trojanowski, J. Q.; Lee, V. M. Y. Neurodegenerative diseases: a decade of discovers paves the way for therapeutic breakthroughs. *Nat. Med.* **2004**, *10*, 1055−1063.

(22) Ballatore, C.; Lee, V. M. Y.; Trojanowski, J. Q. Tau-mediated neurogegeneration in Alzheimer's disease and related disorders. *Nat. Rev. Neurosci.* **2007**, *8*, 663−672.

(23) Dobson, C. M. Protein misfolding, evolution and disease. *Trends Biochem. Sci.* **1999**, *24*, 329−332.

(24) Shcharbin, D.; Pedziewiatr, E.; Bryszewska, M. How to study dendrimers I: Characterization. *J. Controlled Release* **2009**, *135*, 186−197.

(25) Esfand, R.; Tomalia, D. A. Poly(amidoamine) (PAMAM) dendrimers: From biomimicry to drug delivery and biomedical applications. *Drug Discovery Today* **2001**, *6*, 427−436.

(26) Cloninger, M. Biological applications of dendrimers. *Curr. Opin. Chem. Biol.* **2002**, *6*, 742−748.

(27) Svenson, S. Dendrimers as versatile platform in drug delivery applications. *Eur. J. Pharm. Biopharm.* **2009**, *71*, 445−462.

(28) Klajnert, B.; Cortijo-Arellano, M.; Bryszewska, M.; Cladera, J. Influence of heparin and dendrimers on the aggregation of two amyloid peptides related to Alzheimer's and prion diseases. *Biochem. Biophys. Res. Commun.* **2006**, *339*, 577−582.

(29) Jevprasesphant, R.; Penny, J.; Attwod, D.; D'Emanuele, A. Transport of dendrimers nanocarriers thought epithelial cells via the transcellular route. *J. Controlled Release* **2004**, *97*, 259−267.

(30) Kitchens, K. M.; Foraker, A. B.; Kolhatkar, R. B.; Swaan, P. W.; Ghandehari, H. Endocytosis and interaction of poly(aminoamide) dendrimers with Caco-2 cells. *Pharm. Res.* **2003**, *24*, 2138−2145.

(31) El-Sayed, M.; Rhodes, C. A.; Ginski, M.; Ghandehari, H. Transport mechanism(s) of poly(aminoamide) dendrimers across Caco-2 cell monolayers. *Int. J. Pharm.* **2003**, *265*, 151−157.

(32) Klajnert, B.; Stanisławska, L.; Bryszewska, M.; Pałecz, B. Interactions between PAMAM dendrimers and bovine serum albumin. *Biochim. Biophys. Acta* **2003**, *1648*, 115−126.

(33) Klajnert, B.; Cladera, J.; Bryszewska, M. Molecular interactions of dendrimers with amyloid peptides: pH dependence. *Biomacromolecules* **2006**, *7*, 2186−2191.
(34) Supattapone, S.; Wille, H.; Uyechi, L.; Safar, J.; Tremblay, P.; Szoka, F. C.; Cohen, F. E.; Prusiner, S. B.; Scott, M. Branched polyamines cure prion-infected neuroblastoma cells. *J. Virol.* **2001**, *75*, 3453−3461.
(35) Ficher, M.; Appelhans, D.; Voit, B.; Klajnert, B.; Bryszewska, M.; Rogers, M. The influence of surface functionality of poly(propylene imine) dendrimers on aggregation and propagation of scrapie prion protein. *Biomacromolecules* **2010**, *11*, 1314−1325.
(36) Klajnert, B.; Appelhans, D.; Komber, H.; Morgner, N.; Schwarz, S.; Richter, S.; Brutschy, B.; Ionov, M.; Tonkikh, A. K.; Bryszewska, M.; Voit, B. The influence of densely organized maltose shell on the biological properties poly(propylene imine) dendrimers: new effect dependent on hydrogen bonding. *Chem.—Eur. J.* **2008**, *14*, 7030−7041.
(37) Klajnert, B.; Cortijo-Arellano, M.; Cladera., J.; Majoral, J. P.; Caminade, A. M.; Bryszewska, M. Influence of phosphorus dendrimers on the aggregation of the prion peptide PrP 185−208. *Biochem. Biophys. Res. Commun.* **2007**, *364*, 20−25.
(38) Solassol, J.; Crozet, C.; Perrier, V.; Leclaire, J.; Beranger, F.; Caminade, A. M.; Meunier, B.; Dormont, D.; Majoral, J. P.; Lehmann, S. Cationic phosphorus-containing dendrimers reduced prion replication both in cell culture and in mice infected scrapie. *J. Gen. Virol.* **2004**, *85*, 1791−1799.
(39) Caminade, A. M.; Majoral, J. P. Water-soluble phosphorus-containing dendrimers. *Prog. Polym. Sci.* **2005**, *30*, 491−505.
(40) Maszewska, M.; Leclaire, J.; Cieslak, M.; Nawrot, B.; Okruszek, A.; Caminade, A. M.; Majoral, J. P. Water-soluble polycationic dendrimers with a phosphoramidothioate backbone: preliminary studies of cytotoxicities and oligonucleotide/plasmid delivery in human cell culture. *Oligonucleotides* **2003**, *13*, 193−207.
(41) Loup, C.; Zanta, M. A.; Caminade, A. M.; Majoral, J. P.; Meunier, B. Preparation of water-soluble cationic phosphorus-containing dendrimers as DNA transfecting agents. *Chem.—Eur. J.* **1999**, *5*, 3644−3650.
(42) Hedgepeth, C. M.; Conrad, L. J.; Zhang, J.; Huang, H. C.; Lee, V. M.; Klein, P. S. Activation of the Wnt signaling pathway: a molecular mechanism for lithium action. *Dev. Biol.* **1997**, *185*, 82−91.
(43) Bradford, M. M. A rapid and sensitive method for the quantitation of microgram quantities of protein utilizing the principle of protein-dye binding. *Anal. Biochem.* **1976**, *72*, 248−254.
(44) Hansen, M. B.; Nilsen, S. E.; Berg, K. Re-examination and further development of a précis and rapid dye for measuring cell growth/cell kill. *The J. Immunol. Methods* **1989**, *29*, 203−210.
(45) Loveland, B. E.; Johns, T. G.; Mackay, I. R.; Vaillant, F.; Wang, Z. X.; Hertzog, P. J. Validation of the MTT dye assay for enumeration of cells in proliferative and antiproliferative assays. *Biochem. Int.* **1992**, *27*, 501−510.
(46) Mukherjeea, S. P.; Lynga, F. M.; Garciaa, A.; Davorena, M.; Byrneb, H. J. Mechanistic studies of in vitro cytotoxicity of poly(amidoamine) dendrimers in mammalian cells. Toxicology and Applied. *Pharmacology* **2010**, *248/3*, 259−268.
(47) Woody, R. W. Circular dichroism of peptides. In *Conformation in Biology and Drug Design*; Academic Press: New York, 1985; pp 15−114.
(48) Yang, J. T.; Wu, C. C.; Martinez, H. M. Calculation of protein conformation from circular dichroism. *Methods Enzymol.* **1986**, *130*, 208−269.
(49) Bohm, G.; Muhr, R.; Jaenicke, R. Quantitive analysis of protein far UV circular dichroism spectra by neuronal networks. *Protein Eng.* **1992**, *5*, 191−195.
(50) Sreerama, N.; Venyaminov, S. Y.; Woody, R. W. Estimation of peptide secondary structure from circular dichroism spectra: inclusion of denatured peptides with native peptides in the analysis. *Anal. Biochem.* **2000**, *287*, 243−251.
(51) Sreerama, N.; Woody, R. W. Estimation of peptide secondary structure from circular dichroism spectra: comparison of CONTIN, SELCON, and CDSSTR methods with an expanded reference set. *Anal. Biochem.* **2000**, *287*, 252−260.
(52) Pérez, M.; Valpuesta, J. M.; Medina, M.; Montejo de Garcini, E.; Avila, J. Polymerization of tau into filaments in the presence of heparin: the minimal sequence required for tau-tau interaction. *J. Neurochem.* **1996**, *67*, 1183−1190.
(53) Callis, P. R. ^1L_a and ^1L_b transitions of tryptophan: applications of theory and experimental observation to fluorescence of proteins. *Methods Enzymol.* **1997**, *278*, 113−150.
(54) Mahfoud, R.; Garmy, N.; Maresca, M.; Yahi, N.; Puigserver, A.; Fantini, J. Identification of a common shingolipid-binding domain in Alzheimer, prion, and HIV-1 proteins. *J. Biol. Chem.* **2002**, *277*, 11292−11296.
(55) Walsh, D. M.; Klyubin, I.; Foldeeva, J. V.; Rowan, M. J.; Selkoe, D. J. Amyloid-beta oligomers: their production, toxicity and therapeutic inhibition. *Biochem. Soc. Trans.* **2002**, *30*, 534−583.
(56) Iqbal, K.; Alonso Adel, C.; Grundke-Iqbal, I. Cytosolic abnormally hyperphosphorylated tau but not paired helical filaments sequester normal MAPs and inhibit microtubule assembly. *J. Alzheimer Dis.* **2008**, *14*, 365−370.
(57) Goedert, M.; Jakes, R.; Spillantini, M. G.; Hasegawa, M.; Smith, M. J.; Crowther, R. A. Assembly of microtubule-associated protein tau into Alzheimer-like filaments induced by sulphated glycosaminoglycans. *Nature* **1996**, *383*, 550−553.